Research Square

Preprints are preliminary reports that have not undergone peer review.
They should not be considered conclusive, used to inform clinical practice,
or referenced by the media as validated information.

Influence of Spider Silk Reinforcement on the Thermal Stability and Degradation Kinetics of PLA/Starch Biocomposites

Jane Gatwiri Ireri

janegdan@gmail.com

Chuka University

Kamweru Paul Kuria

Chuka University

Martin Mutie

Chuka University

Research Article

Keywords: Biodegradable composites, Polylactic acid (PLA), Starch, Spider silk, Thermal degradation kinetics, Kinetic analysis

Posted Date: August 8th, 2026

DOI: https://doi.org/10.21203/rs.3.rs-10482891/v1

License: This work is licensed under a Creative Commons Attribution 4.0 International License.
Read Full License

Additional Declarations: No competing interests reported.

Influence of Spider Silk Reinforcement on the Thermal Stability and Degradation Kinetics of PLA/Starch Biocomposites

Jane Gatwiri Ireri[1*] Kamweru Paul Kuria[2] Martin Mutie[3]

[*1] janegdan@gmail.com Department of Physical Sciences, Chuka University, Chuka, Kenya

[2] pkamweru@gmail.com Department of Physical Sciences, Chuka University, Chuka, Kenya

[3] martmulesh@gmail.com Department of Physical Sciences, Chuka University, Chuka, Kenya

Abstract

This study investigates the thermal degradation behavior and degradation kinetics of polylactic acid (PLA)/starch biocomposites reinforced with spider silk for sustainable packaging applications. Thermogravimetric analysis (TGA) was conducted under a nitrogen atmosphere at heating rates of 10, 15, and 20 °C min^{-1} to assess the impact of starch and spider silk on the thermal stability of PLA. The results revealed that the addition of starch decreased the thermal stability of PLA, leading to a reduction in the maximum degradation temperature (Tmax) from 386 °C for neat PLA to 369 °C for the PLA/starch blend. In contrast, the incorporation of spider silk enhanced thermal resistance, raising Tmax to 373 °C and 383 °C for composites with 1 wt% and 2 wt% spider silk, respectively. Moreover, spider silk promoted char formation, leading to increased residual mass following degradation. Degradation kinetics were evaluated utilizing the Flynn–Wall–Ozawa (FWO) and Kissinger methods to calculate the apparent activation energy (Ea). FWO analysis demonstrated conversion-dependent activation energies, showing that starch introduced heterogeneous multi-step degradation behavior, whereas spider silk raised the energy barrier for thermal decomposition by enhancing interfacial interactions and limiting chain mobility. Kissinger analysis exhibited a similar trend, validating the enhancement of thermal stability in the composites by spider silk reinforcement. Overall, the results demonstrate that spider silk effectively mitigates the thermally destabilizing effect of starch and serves as a promising bio-reinforcement for the development of thermally stable, biodegradable PLA-based composites suitable for sustainable packaging applications.

Keywords: Biodegradable composites; Polylactic acid (PLA); Starch; Spider silk; Thermal degradation kinetics; Kinetic analysis.

1.1 Introduction

Polylactic acid (PLA) is one of the most widely studied biodegradable polymers derived from renewable resources because of its biodegradability, biocompatibility, low toxicity, good mechanical strength, water-barrier properties, and ease of processing [1- 3]. Despite these advantages, the broader application of PLA in high-performance packaging is constrained by its relatively low thermal resistance, brittleness, slow crystallization rate, and susceptibility to thermal degradation during processing [4]. Thermal degradation of PLA primarily occurs through random chain scission, intra-molecular trans-esterification, and depolymerization reactions when exposed to elevated temperatures. During melt processing, PLA exhibits

a narrow processing window because temperatures required for adequate flow can approach the onset of thermal decomposition [5]. Consequently, prolonged exposure to processing temperatures can reduce molecular weight, deteriorate mechanical properties, and limit service performance in applications requiring thermal stability.

1.1.1 Influence of Starch on Thermal Stability

To improve sustainability and reduce production costs, PLA is frequently blended with starch, a low-cost, abundant, and fully biodegradable polysaccharide [6-7]. Although starch enhances compostability and economic viability, it generally lowers the thermal stability of PLA-based composites. The reduction in thermal stability is largely attributed to the hydrophilic nature of starch and its weak compatibility with the hydrophobic PLA matrix [8-10]. Poor interfacial adhesion promotes phase separation, creating defects that accelerate heat-induced degradation. In addition, starch undergoes dehydration and polysaccharide decomposition at lower temperatures than PLA, generating volatile compounds that initiate further degradation of the surrounding matrix. Without compatibilization or reinforcement, the immiscibility between PLA and starch can result in large crystalline domains and stress concentration sites that facilitate premature failure and accelerate degradation processes [11].

1.1.2 Natural Fiber Reinforcement and the Role of Spider Silk

Natural fiber reinforcement has emerged as an effective strategy for improving the thermal performance of PLA/starch composites while maintaining biodegradability [12- 13]. Among available bio-reinforcements, spider silk has attracted considerable attention because of its exceptional mechanical properties and unique protein structure. Spider silk fibroin consists of highly ordered β-sheet crystalline regions embedded within amorphous domains. These β-sheet crystals provide remarkable structural stability and resistance to thermal deformation, enabling spider silk to contribute positively to composite thermal resistance [14-15]. The presence of β-sheet crystallinity can also promote nucleation and improve crystallization behavior within PLA matrices. Functional groups present in silk proteins facilitate interfacial interactions with both PLA and starch through hydrogen bonding [16], improving stress transfer and thermal stability. Spider silk fibers also act as barriers to volatile degradation products and enhance char formation during thermal decomposition [12, 17].

1.1.3 Thermal Degradation Kinetics of PLA/Starch/Silk Composites

Thermogravimetric analysis (TGA) is commonly employed to investigate degradation behavior and thermal stability of biodegradable composites. The Flynn–Wall–Ozawa (FWO) method is a widely used model-free isoconversional technique for determining activation energy across different stages of decomposition [18]. The Kissinger method estimates activation energy from the maximum degradation rate observed during TGA. Activation energy is an important indicator of thermal stability, with higher values generally reflecting greater resistance to degradation. Variations in activation energy can reveal changes in degradation pathways, interfacial interactions, and decomposition mechanisms. Therefore, kinetic analyses

provide critical insight into how spider silk modifies the thermal degradation behavior of PLA/starch composites.

Although numerous studies have investigated the thermal behavior of PLA, starch-based blends, and silk-reinforced biocomposites, limited information exists concerning the thermal degradation kinetics of PLA/starch composites reinforced with spider silk. Most previous studies have focused on mechanical performance, crystallization, or general thermal stability [19], while the influence of spider silk on degradation mechanisms and activation energy remains poorly understood. Furthermore, limited work has applied Flynn–Wall–Ozawa and Kissinger approaches to evaluate thermal decomposition pathways in PLA/starch/spider silk systems. A comprehensive investigation of thermal degradation behavior and kinetic parameters is therefore required to optimize formulations for sustainable packaging applications.

1.2 Materials and Methods

1.2.1 Materials

Polylactic acid (PLA) pellets were used as the primary polymer matrix. Tapioca starch was selected as the biodegradable filler because of its availability, low cost, and compostability. Spider silk collected from Golden Orb web spiders was used as the natural protein-based reinforcement. Glycerol was used as a plasticizer during thermoplastic starch preparation, while distilled water was used as the processing medium.

1.2.2 Preparation of Thermoplastic Starch–Spider Silk Blends

Thermoplastic starch (TPS) formulations were prepared from starch, distilled water, glycerol, and spider silk. The constituents were weighed according to the formulation design and mixed thoroughly at 80 °C for 10 min to obtain homogeneous blends. The control TPS formulation (TPS-S-0) contained starch, water and glycerol only, while TPS-S-1 and TPS-S-2 contained 1 and 2 wt% spider silk, respectively. Glycerol facilitated starch plasticization and improved blend processability.

1.2.3 Preparation of PLA/TPS and PLA/TPS–Spider Silk Composites

Composite fabrication was carried out in two stages involving melt blending and compression molding. PLA and TPS-based formulations were combined at a fixed PLA:TPS ratio of 70:30. PLA was first melted at 210 °C and subsequently blended with TPS formulations containing different spider silk concentrations. Continuous mixing was maintained for 15 min to ensure uniform dispersion. The melt-blended materials were extruded through manual melt blending and subsequently hot-pressed (compression molded) to obtain homogeneous composite sheets. Four formulations were produced: neat PLA (A), PLA/TPS (B), PLA/TPS/1 wt% spider silk (C), and PLA/TPS/2 wt% spider silk (D). Small specimens (~30 mg) were cut from the molded samples for thermal analysis.

1.2.4 Thermogravimetric Analysis (TGA)

Thermogravimetric analysis was conducted using a Shimadzu TGA-50 thermogravimetric analyzer to evaluate the thermal stability and degradation characteristics of neat PLA and the prepared composites.

Approximately 5–10 mg of each specimen was placed in a 13 mg aluminum sample pan, ensuring that the combined pan and sample mass did not exceed 30 mg. Thermal degradation experiments were performed under a nitrogen atmosphere to eliminate oxidative degradation. Nitrogen was supplied at a constant flow rate of 50 mL min−1 throughout the experiment. Samples were heated from ambient temperature to 600 °C at heating rates of 10, 15, and 20 °C min−1. The mass loss was continuously recorded as a function of temperature to generate thermogravimetric (TG) curves.

1.2.5 Derivative Thermogravimetric (DTG) Analysis

Derivative thermogravimetric (DTG) curves were obtained by differentiating the TG data with respect to temperature. DTG analysis was used to determine the maximum degradation rate and corresponding peak degradation temperature (Tmax). The DTG peaks were used to identify degradation stages and assess the influence of spider silk reinforcement on decomposition behavior and thermal stability.

1.2.6 Flynn–Wall–Ozawa (FWO) Kinetic Analysis

Thermal degradation kinetics was evaluated using the model-free Flynn–Wall–Ozawa (FWO) isoconversional method. The conversion degree α is calculated as;

$$\alpha = \frac{m_0 - m_t}{m_0 - m_f} \quad \text{(1.1)}$$

Where, where m_0, m_t, and m_f were the initial mass, mass at time t and the final mass of the samples respectively, from Arrhenius equation, the decomposition rate is described by the equation:

$$\frac{d\alpha}{dt} = AE^{(\frac{E\alpha}{RT})} f(\alpha) \quad \text{(1.2)}$$

where, A is the pre-exponential factor, E_α is the activation energy, R is the gas constant and T is the absolute temperature of reaction.

When the heating rate β is introduced, equation 1.2 transforms into non- isothermal expressed as;

$$\frac{d\alpha}{dt} = \frac{A}{\beta} E^{(\frac{E\alpha}{RT})} f(\alpha) \quad \text{(1.3)}$$

On integration, equation 4.4 becomes

$$g(\alpha) = \int_0^\alpha \frac{d\alpha}{f(\alpha)} = \frac{A}{\beta} \int_{T_0}^{T} E^{(\frac{E\alpha}{RT})} dT = \frac{AE\alpha}{\beta R} P(x) \quad \text{(1.4)}$$

Where g(α) is the integral form of the conversion dependence function f(α), and P(x) is an approximation.

The thermal degradation kinetic at each conversion degree (α) was calculated using Flynn-Wall-Ozawa (FWO) method with the equation;

$$\log \beta = log \frac{AE\alpha}{Rg(\alpha)} - 2.135 - \frac{0.4567E\alpha}{RT} \quad \text{(1.5)}$$

Taking α as a constant, E_α can be calculated form the slope given by 0.4567 E_α /RT.

For a fixed conversion level, activation energy (Eα) was determined from the slope of plots of logβ against 1/T. The method enables determination of activation energy as a function of conversion without assuming a reaction mechanism [20].

1.2.7 Kissinger Kinetic Analysis

The Kissinger method was applied using peak temperatures obtained from DTG curves. The method relates heating rate and peak degradation temperature according to:

$$\ln\left(\frac{\beta}{T^2}\right) = \ln\left(\frac{AR}{\mathrm{E}\alpha}\right) - \frac{\mathrm{E}\alpha}{R\mathrm{T}_{max}} \quad \text{..... (1.6)}$$

Activation energy was calculated from the slope of a plot of ln(β/Tmax²) versus 1/Tmax. The Kissinger approach provides single apparent activation energy associated with the maximum degradation rate and was used to compare the thermal resistance of the different composite formulations.

1.3 Results

1.3.1 Thermal Degradation Behaviour of PLA and Its Composites

Thermogravimetric analysis (TGA) was conducted under nitrogen at heating rates of 10, 15 and 20 °C min⁻¹ to evaluate the thermal stability of neat PLA, PLA/starch, PLA/starch/1% spider silk and PLA/starch/2% spider silk composites. The corresponding TG curves are presented in Fig 1, while the DTG curves are presented in Fig 2.

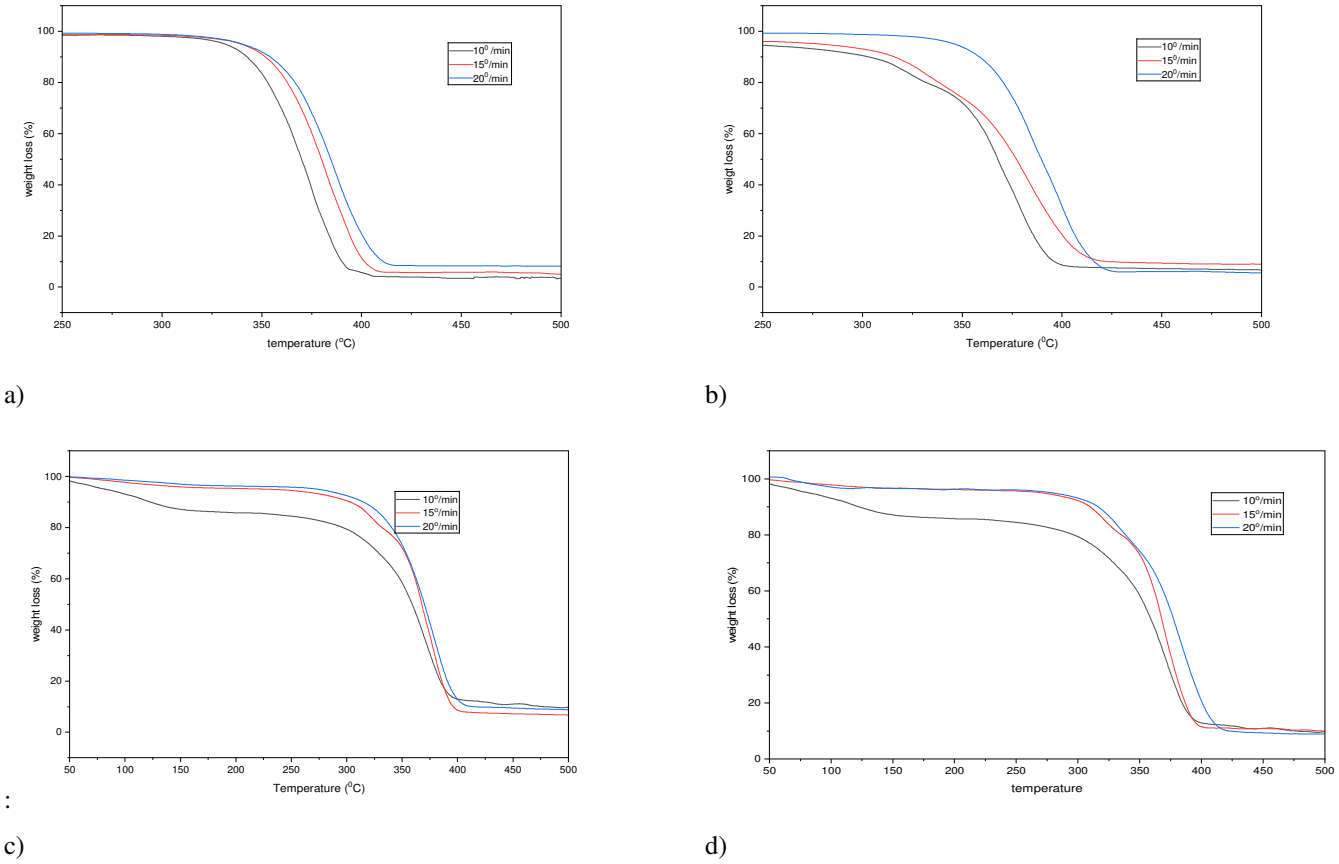


Fig 1 TG curves of (a) PLA, (b) PLA/starch, (c) PLA/starch/1% spider silk and (d) PLA/starch/2% spider silk at heating rates of 10, 15 and 20 °C min⁻¹ under nitrogen atmosphere.

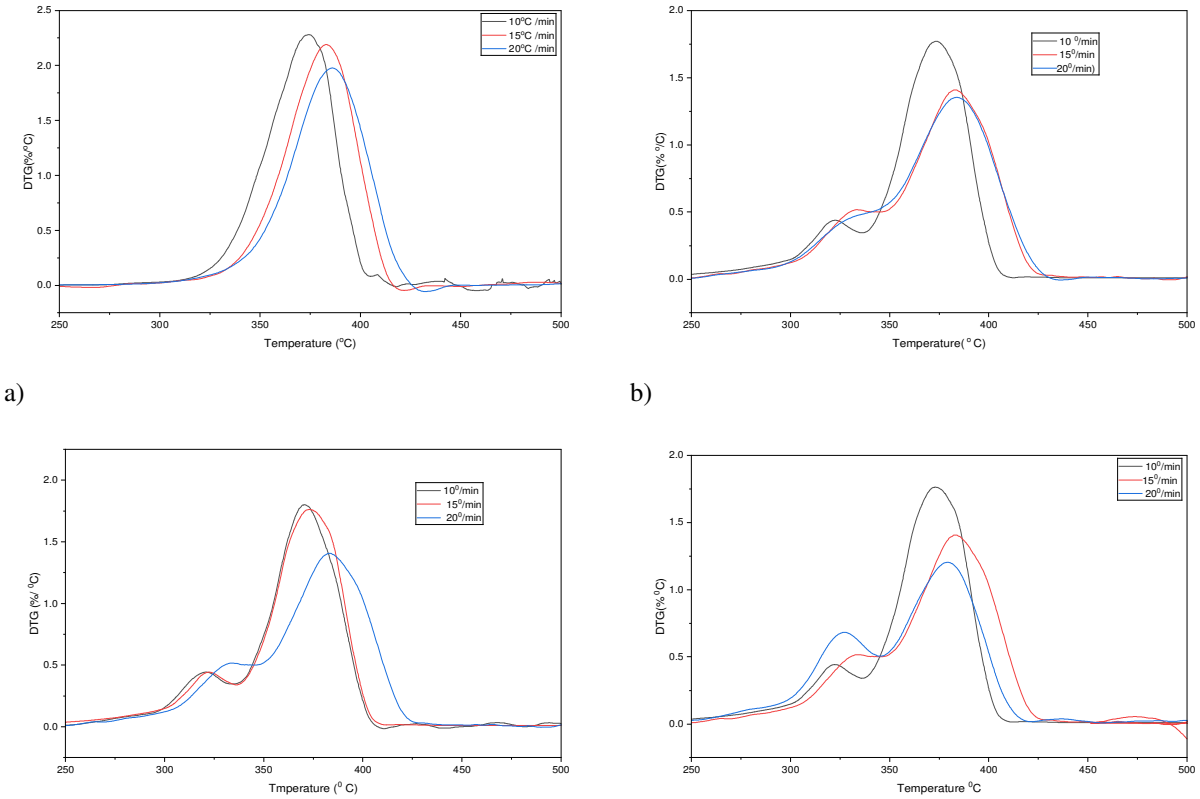


Fig 2 DTG curves of (a) PLA, (b) PLA/starch, (c) PLA/starch/1% spider silk and (d) PLA/starch/2% spider silk at heating rates of 10, 15 and 20 °C min^{-1} under nitrogen atmosphere.

Neat PLA exhibited a single dominant degradation stage characteristic of random chain scission, depolymerization and intramolecular transesterification reactions. In contrast, PLA/starch composites exhibited multi-step degradation due to overlapping decomposition of starch and PLA components. The incorporation of spider silk shifted both Tonset and Tmax to higher temperatures relative to PLA/starch, indicating improved thermal stability through enhanced intermolecular interactions, hydrogen bonding and restricted diffusion of volatile degradation products. The extracted thermal degradation parameters including onset temperature (T_{onset}), maximum degradation temperature (T_{max}), and residual weight (W(R)) are summarized in Table 1.

Table 1: Thermal degradation parameters of PLA and its composites

Sample	Tonset (°C)	Tmax (°C)	Residual Char (%)
PLA	289	386	3.0
PLA/starch	275	369	5.4
PLA/starch/1% silk	283	373	6.3
PLA/starch/2% silk	286	383	7.4

Neat PLA showed the highest thermal stability, exhibiting Tonset and Tmax values of 289 and 386 °C, respectively. Incorporation of starch reduced thermal stability since starch degrades at lower temperatures and introduces weak interfacial regions within the blend. The addition of spider silk progressively restored thermal stability. At 2 wt% spider silk, composite displayed a Tmax of 383 °C, approaching that of neat PLA, while also producing the highest char yield (7.4%), indicating enhanced thermal resistance and carbonization behaviour. The low residual char (3.0%) confirms that PLA undergoes almost complete volatilization under nitrogen, consistent with its aliphatic polyester structure and limited char-forming tendency [21].

For all formulations, increasing the heating rate shifted the TG and DTG profiles toward higher temperatures. This behaviour is attributed to thermal lag, whereby heat transfer into the sample becomes less efficient at higher heating rates, causing decomposition reactions to occur at apparently higher temperatures. Similar behaviour has been reported for biodegradable polymers and polymer composites. The progressive increase in onset degradation temperature (Tonset) and maximum degradation temperature (Tmax) confirms the kinetic dependence of the degradation process.

1.3.2 Kinetic Analysis

1.3.3 Flynn–Wall–Ozawa (FWO) Analysis

The degradation kinetics of PLA and its composites were evaluated using the Flynn–Wall–Ozawa iso-conversional method. TGA measurements were conducted at multiple heating rates; 10^{o}C /min, 15^{o}C /min and 20^{o}C /min, and the temperatures corresponding to fixed degrees of conversion were extracted. Linear plots of log (β) versus 1/T exhibited good linearity ($R^2 > 0.97$),), indicating applicability of the isoconversional approach.

For neat PLA (Fig 3(a)), the FWO plots at various degrees of conversion (α = 0.1–0.9) typically produce nearly parallel straight lines, indicating that the thermal degradation proceeds via a single dominant reaction mechanism [22]. However, the calculated apparent activation energy values generally increases slightly with increasing α, indicating that although the degradation proceeds through a single dominant

reaction mechanism, higher thermal energy is required as degradation advances. At the initial stages (α = 0.1–0.3), less activation energy is required in the breakdown of less stable amorphous regions with higher chain mobility, whereas at higher conversions the reaction shifts toward the decomposition of more ordered and crystalline domains. At α = 0.7–0.9 chains are more tightly packed and stabilized by stronger intermolecular interactions, thereby restricting segmental motion and increasing resistance to bond cleavage, hence the rise in activation energy reflecting increasing structural stability of the material. This confirms homogeneous structural behavior and uniform thermal decomposition [23].

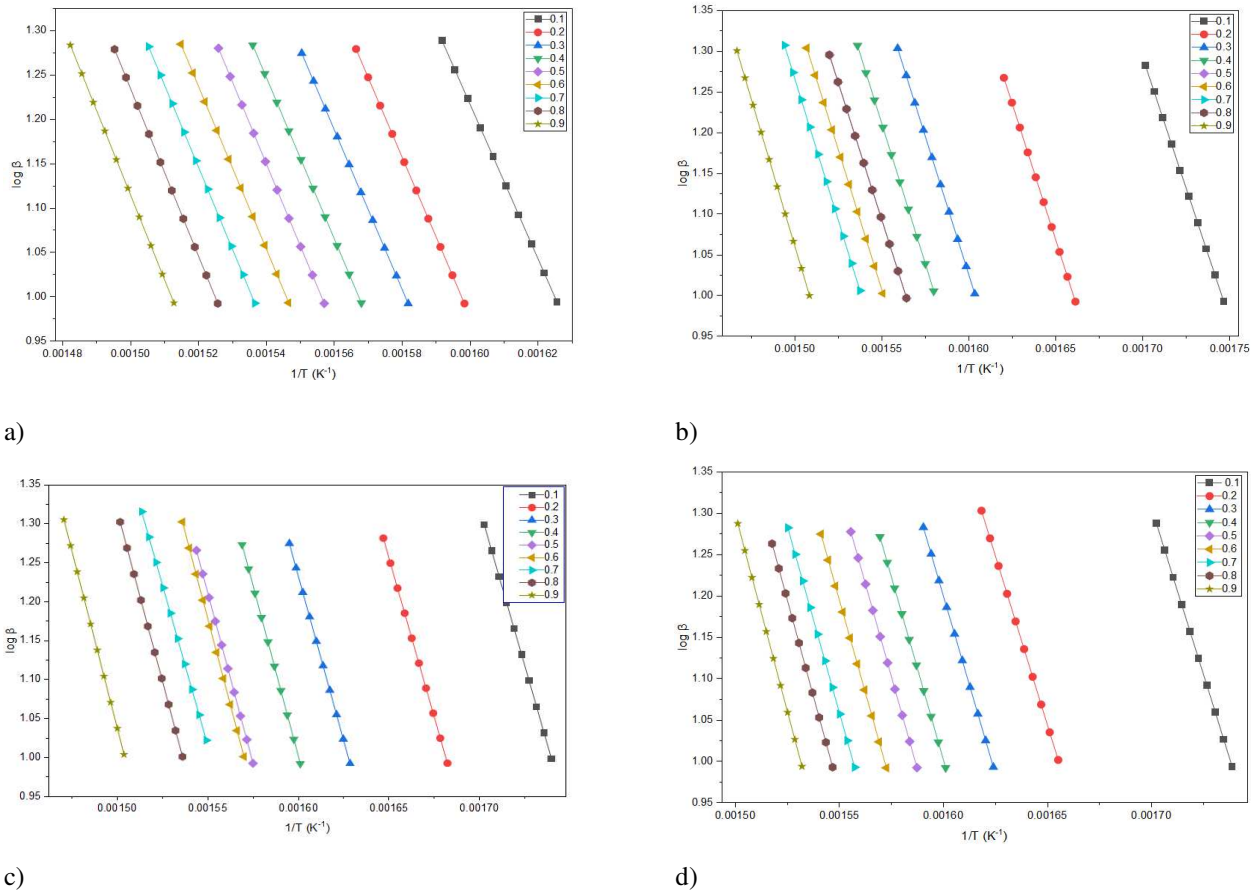


Fig 3 FWO curves at varying degree of conversion (a) PLA, (b) PLA/starch, (c) starch/PLA/ 1% spider silk and (d) starch/PLA/ 2% spider silk

When starch is added into PLA (Fig 3b), the FWO curves deviate from parallelism as the degree of conversion increases, and the slopes of the log (β) versus 1/T plots change noticeably with α, demonstrating that the apparent activation energy is strongly conversion-dependent. It also indicates the presence of multiple overlapping degradation processes arising from the thermally less stable starch phase and the relatively more stable PLA matrix [24] The lower E_α values observed at lower conversion levels correspond to starch dehydration and depolymerization, while higher E_α values emerge at intermediate and higher

conversion levels where PLA chain scission becomes dominant, confirming heterogeneous and multi-step degradation behavior in PLA/starch blend [24] [25]

For PLA/starch/spider silk composites (Fig c and d), the FWO curves also exhibit conversion-dependent behavior due to the complexity of the ternary system. When spider silk is well dispersed and effectively bonded within the matrix, the slopes of the FWO plots generally become steeper compared to those of the PLA/starch blend, resulting in higher apparent activation energy values across most conversion levels, particularly in the mid-to-high α range as reported by [26]. From the FWO results in Table 2, neat PLA exhibited the highest activation energy, compared to PLA/starch/spider silk, where PLA/starch displayed the lowest activation energy.

Table 2: Activation energy (E_α) obtained from the FWO method

	α	0.1	0.2	0.3	0.4	0.5	0.6	0.7	0.8	0.9
PLA	E_α	158	163	164	165	168	167	168	171	173
	R^2	0.9885	0.9697	0.9577	0.9798	0.9720	0.9834	0.9760	0.9691	0.9764
PLA/starch	E_α	117	121	123	125	122	125	126	127	131
	R^2	0.9775	0.9376	0.9992	0.9956	0.9973	0.9889	0.9956	0.9951	0.9999
PLA/starch/0.1 spider silk	E_α	147	148	153	156	159	162	150	159	165
	R^2	0.994	0.9754	0.9586	0.928	0.9333	0.9907	0.9548	0.9999	0.9978
PLA/starch/0.2 spider silk	E_α	147	148	157	159	163	163	164	167	173
	R^2	0.9872	0.9994	0.9782	0.9494	0.9659	0.9587	0.9771	0.9813	0.9869

The overall activation-energy trend was PLA > PLA/starch/2% silk > PLA/starch/1% silk > PLA/starch, demonstrating the beneficial effect of spider silk reinforcement on thermal stability.

1.3.4 Kissinger Analysis

The Kissinger method was used to determine the apparent activation energy at the maximum degradation rate. The results are summarized in Table 3.

Table 3 Kissinger kinetic parameters for PLA and its composites

Sample	Slope (-Eα/R)	Eα (kJ mol^{-1})	R^2
PLA	-22225	184	0.964
PLA/starch	-17669	146	0.963
PLA/starch/1% silk	-18958	157	0.966
PLA/starch/2% silk	-25949	215	0.9998

Kissinger activation energies were generally higher than those obtained using the FWO method since Kissinger analysis evaluates the dominant degradation stage at Tmax and assumes a single-step mechanism. Nevertheless, both methods showed the same overall trend, with PLA/starch displaying the lowest activation energy and spider silk reinforcement increasing the resistance of the composites to thermal degradation.

1.4 Discussion

The thermogravimetric results demonstrate that spider silk is not merely inert filler but an active thermally stabilizing reinforcement capable of modifying the degradation behaviour of PLA/starch composites. The decline in thermal stability observed after starch incorporation is expected because starch possesses lower thermal resistance than PLA and introduces heterogeneous interfaces that facilitate heat-induced degradation. This is evidenced by the reduction in Tonset from 289 °C for neat PLA to 275 °C for PLA/starch and the decrease in Tmax from 386 °C to 369 °C. However, incorporation of spider silk progressively reversed this deterioration, increasing Tonset to 283–286 °C and Tmax to 373–383 °C. The ability of spider silk to recover thermal stability is significant because natural fibre reinforcements commonly improve mechanical properties but often provide only limited thermal enhancement. In the present system, spider silk simultaneously improved thermal resistance and char-forming behaviour, demonstrating its multifunctional reinforcing capability [14, 27]

A primary mechanism responsible for the enhanced thermal stability is the unique hierarchical protein structure of spider silk. Spider silk fibroin contains highly ordered β-sheet nanocrystalline domains embedded within amorphous protein regions. These β-sheet crystals act as thermally stable structural domains that require greater energy for disruption than the surrounding polymer matrix [28-29]. The exceptional stability of β-sheet-rich silk structures has been associated with extensive intermolecular hydrogen bonding and tightly packed molecular arrangements that restrict thermal motion and delay bond cleavage. β-sheet crystalline regions are recognised as the principal source of the remarkable strength, toughness and structural stability of spider silk materials, and their presence can increase resistance to thermal degradation in polymer composites [30]. Spider silk also improves thermal resistance through interfacial interactions with both PLA and starch. The silk protein contains amide, carboxyl and amino

functional groups capable of forming hydrogen bonds with carbonyl groups in PLA and hydroxyl groups in starch [31]. These intermolecular interactions improve interfacial adhesion between the hydrophobic PLA phase and hydrophilic starch phase. Improved compatibility reduces interfacial defects, microvoids and weak domains that normally act as preferential initiation sites for thermal decomposition [32]. Consequently, greater thermal energy is required to initiate degradation in spider-silk-reinforced composites than in the PLA/starch blend. This explanation is supported by the observed increase in activation energy obtained from both Flynn–Wall–Ozawa and Kissinger analyses.

Another important stabilization mechanism arises from the barrier effect created by dispersed spider silk fibres. During thermal decomposition, degradation products must diffuse through the composite before volatilization occurs. The silk fibres create a tortuous diffusion pathway that slows the escape of volatile products and delays overall mass loss [22]. The delayed release of volatile decomposition products reduces degradation propagation and contributes to higher Tmax values. This phenomenon explains why the 2 wt% spider silk composite exhibited degradation temperatures approaching those of neat PLA despite containing a thermally less stable starch phase

The increase in residual char from 5.4% for PLA/starch to 7.4% for PLA/starch/2% spider silk further demonstrates the role of silk in promoting thermal stability. Protein-based materials frequently undergo carbonization reactions during pyrolysis, producing stable carbonaceous residues. Spider silk contributes nitrogen-containing protein structures that favour char formation and stabilization [33]. The resulting char layer functions as a protective thermal shield, reducing heat transfer to the underlying material and slowing further degradation. The higher char yields observed in the silk-reinforced composites therefore indicate enhanced resistance to complete thermal decomposition.

The kinetic analysis provides additional evidence of the stabilizing role of spider silk. The FWO results showed progressively increasing activation energy with increasing silk content, particularly at intermediate and high conversion levels where degradation of the more stable polymer fractions dominates. Higher activation energy indicates that additional energy is required to break the intermolecular network created by interactions among PLA, starch and spider silk. Similarly, Kissinger activation energies increased from 146 kJ mol−1 for PLA/starch to 157 and 215 kJ mol−1 for the 1% and 2% spider silk composites, respectively. These results confirm that spider silk modifies the degradation pathway by increasing resistance to thermal decomposition.

1.5 Conclusion

Thermogravimetric analysis demonstrated that increasing the heating rate from 10 to 20 °C min^{-1} shifted the degradation profiles of PLA, PLA/starch, and PLA/starch/spider silk biocomposites toward higher temperatures because of thermal lag and kinetic effects. Neat PLA exhibited a predominantly single-step degradation process, whereas the incorporation of starch introduced a more complex multi-step degradation behavior associated with the individual decomposition of starch and PLA components. The addition of

starch reduced the thermal stability of PLA, as evidenced by the decrease in both onset degradation temperature (Tonset) and maximum degradation temperature (Tmax). The incorporation of spider silk effectively mitigated this reduction in thermal stability. Composites reinforced with spider silk exhibited higher Tonset, Tmax, and residual char content compared with the PLA/starch blend. The improvement was most pronounced at 2 wt% spider silk loading, where Tmax approached that of neat PLA, indicating enhanced thermal resistance. This behavior is attributed to improved interfacial hydrogen bonding, restricted polymer chain mobility, and the formation of a semi-interpenetrating network structure that delayed the release of volatile degradation products and promoted char formation.

Kinetic analysis using the Flynn–Wall–Ozawa (FWO) and Kissinger methods further confirmed the influence of composite composition on degradation behavior. Neat PLA displayed nearly constant activation energy values throughout degradation, consistent with a relatively homogeneous single-step mechanism. In contrast, PLA/starch composites exhibited conversion-dependent activation energies, reflecting heterogeneous and multi-stage degradation processes. The addition of spider silk increased the apparent activation energy, particularly at higher conversion levels, indicating greater resistance to thermal decomposition and stronger intermolecular interactions within the composite matrix. Overall, spider silk proved to be an effective bio-reinforcement for PLA/starch composites, enhancing thermal stability, increasing the energy barrier to degradation, and improving char-forming ability. These findings highlight the potential of spider silk-reinforced PLA/starch biocomposites as sustainable packaging materials with improved thermal performance and structural integrity.

1.6 Refences

[1] S. Temesgen, L. Großmann, T. Tesfaye, I. Kuehnert, N. Smolka, and M. Nase, "Rheological, structural and melt spinnability study on thermo-plastic starch/PLA blend biopolymers and tensile, thermal and structural characteristics of melt spun fibers," *J Res Updat. Polym Sci*, vol. 13, pp. 187–209, 2024.

[2] K. Martinez Villadiego, M. J. Arias Tapia, J. Useche, and D. Escobar Macías, "Thermoplastic starch (TPS)/polylactic acid (PLA) blending methodologies: A review," *J. Polym. Environ.*, vol. 30, no. 1, pp. 75–91, 2022.

[3] M. Zorah *et al.*, "Review of the green composite: importance of biopolymers, uses and challenges," *J. Adv. Res. Fluid Mech. Therm. Sci.*, vol. 111, no. 1, pp. 194–216, 2023.

[4] R. E. Drumright, P. R. Gruber, and D. E. Henton, "Polylactic acid technology," *Adv. Mater.*, vol. 12, no. 23, pp. 1841–1846, 2000.

[5] I. Velghe, B. Buffel, V. Vandeginste, W. Thielemans, and F. Desplentere, "Review on the Degradation of Poly (lactic acid) during Melt Processing," *Polymers*, vol. 15, no. 9, p. 2047, 2023.

[6] R. Acioli-Moura and X. S. Sun, "Thermal degradation and physical aging of poly (lactic acid) and its blends with starch," *Polym. Eng. Sci.*, vol. 48, no. 4, pp. 829–836, 2008.

[7] V. Goetjes, J. Zarges, and H. Heim, "Resistance of poly (lactic acid)/starch composites to weathering effects," *J. Appl. Polym. Sci.*, vol. 141, no. 2, p. e54768, 2024.

[8] L. Averous and N. Boquillon, "Biocomposites based on plasticized starch: thermal and mechanical behaviours," *Carbohydr. Polym.*, vol. 56, no. 2, pp. 111–122, 2004.

[9] M. A. Huneault and H. Li, "Morphology and properties of compatibilized polylactide/thermoplastic starch blends," *Polymer*, vol. 48, no. 1, pp. 270–280, 2007.

[10] G. Gamon, P. Evon, and L. Rigal, "Twin-screw extrusion impact on natural fibre morphology and material properties in poly (lactic acid) based biocomposites," *Ind. Crops Prod.*, vol. 46, pp. 173–185, 2013.

[11] G. Kfoury *et al.*, "Recent advances in high performance poly (lactide): from 'green' plasticization to super-tough materials via (reactive) compounding," *Front. Chem.*, vol. 1, p. 32, 2013.

[12] H.-Y. Cheung, K.-T. Lau, X.-M. Tao, and D. Hui, "A potential material for tissue engineering: Silkworm silk/PLA biocomposite," *Compos. Part B Eng.*, vol. 39, no. 6, pp. 1026–1033, 2008.

[13] C. Ferri *et al.*, "MiR-423-5p prevents MALAT1-mediated proliferation and metastasis in prostate cancer," *J. Exp. Clin. Cancer Res.*, vol. 41, no. 1, p. 20, 2022.

[14] D. Hazarika, A. Kumar, and V. Katiyar, "Structural evolution of in situ polymerized poly (L-lactic acid) nanocomposite for smart textile application," *Sci. Rep.*, vol. 12, no. 1, p. 14724, 2022.

[15] J. M. Ferri, M. Aldas, E. Rayon, M. D. Samper, and A. A. Lozano-Pérez, "The influence of different sustainable silk-based fillers on the thermal and mechanical properties of polylactic acid composites," *Polymers*, vol. 14, no. 22, p. 5016, 2022.

[16] F. Wang, Y. Li, C. R. Gough, Q. Liu, and X. Hu, "Dual-crystallizable silk fibroin/poly (L-lactic acid) biocomposite films: Effect of polymer phases on protein structures in protein-polymer blends," *Int. J. Mol. Sci.*, vol. 22, no. 4, p. 1871, 2021.

[17] I. Oliver, J. A. Conesa, and A. Fullana, "Thermal decomposition of bio-based plastic materials," *Molecules*, vol. 29, no. 13, p. 3195, 2024.

[18] R. Venkatesan, M. M. Alrashed, A. A. Vetcher, and S.-C. Kim, "Next-Generation food packaging: progress and challenges of Biopolymer-Based materials," *Polymers*, vol. 17, no. 17, p. 2299, 2025.

[19] D. Mileva, D. Tranchida, and M. Gahleitner, "Designing polymer crystallinity: An industrial perspective," *Polym. Cryst.*, vol. 1, no. 2, p. e10009, 2018.

[20] H. Mahmood, A. Shakeel, A. Abdullah, M. I. Khan, and M. Moniruzzaman, "A comparative study on suitability of model-free and model-fitting kinetic methods to non-isothermal degradation of lignocellulosic materials," *Polymers*, vol. 13, no. 15, p. 2504, 2021.

[21] K. Papadopoulou *et al.*, "Synthesis and characterization of PLA/biochar bio-composites containing different biochar types and content," *Polymers*, vol. 17, no. 3, p. 263, 2025.

[22] R. Patwa, M. Singh, A. Kumar, and V. Katiyar, "Kinetic modelling of thermal degradation and non-isothermal crystallization of silk nano-discs reinforced poly (lactic acid) bionanocomposites," *Polym. Bull.*, vol. 76, no. 3, pp. 1349–1382, 2019.

[23] M. Reit, N. Krug, J. Zarges, and H. Heim, “Evaluation of the Activation Energy for Pyrolytic Degradation of Poly-L-Lactide (PLA) During Artificially Accelerated Aging,” *Biopolymers*, vol. 116, no. 1, p. e23642, 2025.

[24] R. R. M. de Freitas, K. P. do Carmo, F. A. de Pádua, and V. R. Botaro, “Kinetics, thermodynamics and structure: an analysis of corn starch acetylation,” *Mater. Res.*, vol. 28, p. e20240333, 2025.

[25] S. Lv, Y. Zhang, and H. Tan, “Thermal and thermo-oxidative degradation kinetics and characteristics of poly (lactic acid) and its composites,” *Waste Manag.*, vol. 87, pp. 335–344, 2019.

[26] A. K. Maurya, F. M. de Souza, T. Dawsey, and R. K. Gupta, “Biodegradable polymers and composites: Recent development and challenges,” *Polym. Compos.*, vol. 45, no. 4, pp. 2896–2918, 2024.

[27] M. Mansourieh, S. Farshbaf Taghinezhad, A. Abbasi, Y. Chen, and D. Devine, “A study on the degradability and mechanical–rheological correlations of PLA/Silk composites,” *J. Compos. Sci.*, vol. 8, no. 10, p. 428, 2024.

[28] M. Balaraman and N. B. Thamba, “Unravelling the mysteries of spider silk: A comprehensive review of its properties and applications,” *Proc. Inst. Mech. Eng. Part J. Mater. Des. Appl.*, p. 14644207251386702, 2025.

[29] D. Yarger, S. Stoev, and T. Hsing, “A functional-data approach to the Argo data,” *Ann. Appl. Stat.*, vol. 16, no. 1, pp. 216–246, 2022.

[30] N. J.-A. Chan *et al.*, “Spider-silk inspired polymeric networks by harnessing the mechanical potential of β-sheets through network guided assembly,” *Nat. Commun.*, vol. 11, no. 1, p. 1630, 2020.

[31] W. Phasayavan *et al.*, “Silk sericin as a functional biopolymer: From polymer chemistry to biomedical translation,” *Polym. Int.*, 2026.

[32] S. Ren, D. Fan, Q. Zhang, Y. Jiao, J. Xu, and J. Xie, “Fabrication of flame retardant toughened PLA base 3D printed materials with modified lignin by phytic acid,” *RSC Adv.*, vol. 15, no. 45, pp. 38294–38306, 2025.

[33] H. Kim, J. Yoon, H. W. Kwak, and H.-J. Jin, “From Nature to Energy: The Role of Silk in Enhancing Advanced Energy Storage Technologies,” *Fibers Polym.*, vol. 26, no. 8, pp. 3245–3265, 2025.